

Synthesis and DNA-binding Properties of a Cationic Seven-coordinate Manganese(II) Complex Formed with the Tripodal Ligand Tris(*N*-methylbenzimidazol-2-ylmethyl)amine and Salicylate

Huilu Wu, Ying Bai, Jingkun Yuan, Hua Wang, Guolong Pan, Gangqiang Yu, and Xingbin Shu

School of Chemical and Biological Engineering, Lanzhou Jiaotong University, Lanzhou 730070, P. R. China

Reprint requests to Prof. Huilu Wu. E-mail: wuhuilu@163.com

Z. Naturforsch. **2012**, *67b*, 819–826 / DOI: 10.5560/ZNB.2012-0082

Received March 20, 2012

A ternary cationic Mn(II) complex with the tripodal ligand tris(2-(*N*-methyl)benzimidazolylmethyl)amine (Mentb), salicylate and DMF as ligands and nitrate as counterion, [Mn(Mentb)(salicylate)DMF](NO₃), was synthesized and characterized by physico-chemical and spectroscopic methods. The crystal structure of the Mn(II) complex has been determined by single-crystal X-ray diffraction and revealed that the central Mn(II) atom is seven-coordinated. The DNA-binding properties of the Mn(II) complex were investigated by spectrophotometric methods and viscosity measurements, and the results suggest that the Mn(II) complex binds to DNA *via* an intercalation binding mode. Additionally, the complex exhibited potential hydroxyl radical scavenge properties in *in vitro* studies.

Key words: Manganese(II) Nitrate Complex, Crystal Structure, DNA-binding Properties, Tris(2-(*N*-methyl)benzimidazolylmethyl)amine (Mentb)

Introduction

DNA is generally the primary intracellular target of anticancer drugs. The interaction between small molecules and DNA can often cause DNA damage in cancer cells, blocking the division of cancer cells and resulting in cell death [1, 2]. Transition metal complexes are used to bind and react at specific sequences of DNA for finding novel chemotherapeutics, probing DNA and developing highly sensitive diagnostic agents [3, 4]. Manganese is an essential element in the human body. It plays an important role in many biological systems including photosystem II (water oxidation), catalase (disproportionation of hydrogen peroxide), and superoxide dismutase (dismutation of superoxide radicals) [5–7]. Research on how Mn(II) complexes interact with DNA is expected to help in the development of relevant drugs.

Benzimidazole can function as a ligand toward transition metals in a variety of biologically important molecules [8]. Benzimidazoles are known

for their potential to poison DNA topoisomerases or to stabilize complexes of DNA topoisomerases that ultimately result in strand cleavage [9, 10]. In previous work we reported on the perchlorate of a cationic Mn(II) complex with tris(2-(*N*-methyl)benzimidazolylmethyl)amine (Mentb), salicylate, and DMF as ligands [11, 12]. Now we give a full account on the synthesis, crystal structure and DNA-binding properties of the respective nitrate salt of the Mn(II) complex.

Experimental Section

Materials and physical measurements

All chemicals used were of analytical grade. Ethidium bromide (EB) and calf thymus DNA (CT-DNA) were purchased from Sigma and used without further purification. All the experiments involving interaction of the ligand and the complex with CT-DNA were carried out in doubly distilled water with a buffer containing 5 mM Tris and 50 mM NaCl and adjusted to pH = 7.2 with hydrochloric acid. A solution

of CT-DNA gave a ratio of UV absorbance at 260 and 280 nm of about 1.8–1.9, indicating that the CT-DNA was sufficiently free of protein [13]. The CT-DNA concentration per nucleotide was determined spectrophotometrically by employing an extinction coefficient of $6600 \text{ L mol}^{-1} \text{ cm}^{-1}$ at 260 nm [14].

C, H, and N contents were determined using a Carlo Erba 1106 elemental analyzer. The IR spectra were recorded in the $4000\text{--}400 \text{ cm}^{-1}$ region with a Nicolet FI-VERTEX 70 spectrophotometer using KBr pellets. Electronic spectra were taken on Lab-Tech UV Bluestar and Spectrumbab 722sp spectrophotometers. The fluorescence spectra were performed on a LS-45 spectrofluorophotometer at room temperature. Viscosity experiments were conducted on an Ubbelohde viscometer, immersed in a thermostated water bath maintained at $25 \pm 0.1 \text{ }^\circ\text{C}$.

Preparation of

tris(2-(N-methyl)benzimidazolmethyl)amine (Mentb)

Mentb was synthesized by literature methods [15]. Yield: 4.62 g (51 %). M. p.: $215\text{--}217 \text{ }^\circ\text{C}$. – Analysis for $\text{C}_{27}\text{H}_{27}\text{N}_7$: calcd. C 72.14, H 6.05, N 21.81; found C 72.27, H 6.17, N

21.03. – UV/Vis: $\lambda = 279, 289 \text{ nm}$. – FT-IR (KBr): $\nu = 1288$ (C–N); 1477 (C=N); 1614 (C=C) cm^{-1} [16, 17].

Preparation of $[\text{Mn}(\text{Mentb})(\text{salicylate})\text{DMF}](\text{NO}_3)$

To a stirred solution of Mentb (0.449 g, 1 mmol) in hot MeOH (10 mL) $\text{Mn}(\text{NO}_3)_2$ (0.358 g, 1 mmol) in MeOH (5 mL) was added, and subsequently sodium salicylate (0.160 g, 1 mmol) in hot MeOH (5 mL). A colorless product formed rapidly. The precipitate was filtered off, washed with MeOH and absolute Et_2O , and dried *in vacuo*. The dried precipitate was dissolved in DMF to form a colorless solution into which Et_2O was allowed to diffuse at room temperature. Colorless crystals suitable for X-ray measurement were obtained after three weeks. Yield: 0.454 g (47 %). – Analysis for $\text{C}_{37}\text{H}_{39}\text{MnN}_9\text{O}_7$: calcd. C 49.34, H 3.90, N 16.92; found C 50.47, H 4.08, N 16.76. – UV/Vis: $\lambda = 260, 279 \text{ nm}$. – FT-IR (KBr): $\nu = 1250$ $\nu(\text{C-N})$; 1458 $\nu(\text{C=N})$; 1626 $\nu(\text{C=C})$; 1593 $\nu_{\text{as}}(\text{O-C-O})$; 1488 $\nu_{\text{s}}(\text{O-C-O})$; 1388 $\nu(\text{N-O}) \text{ cm}^{-1}$.

X-Ray crystal structure determination

A suitable single crystal was mounted on a glass fiber. The intensity data were collected on a Bruker Smart CMN

	$[\text{Mn}(\text{Mentb})(\text{salicylate})\text{DMF}](\text{NO}_3)$
Molecular formula	$\text{C}_{37}\text{H}_{39}\text{MnN}_9\text{O}_7$
Molecular weight	776.71
Color	colorless
Crystal size, mm^3	$0.40 \times 0.38 \times 0.30$
Crystal system	triclinic
Space group	$P\bar{1}$
a , Å	10.468(5)
b , Å	12.564(6)
c , Å	15.209(8)
α , deg	84.425(5)
β , deg	76.049(5)
γ , deg	77.667(6)
V , Å^3	1894.3(16)
Z	2
$D_{\text{calcd.}}$, g cm^{-3}	1.36
$F(000)$	810
θ range data collection, deg	2.19–26.00
hkl range (max / min)	–12 / 12, –15 / 14, –18 / 18
Reflections collected / independent	14309 / 7285
R_{int}	0.0381
Data / restraints / ref. parameters	7285 / 29 / 493
Final R_1 / wR_2 [$I > 2 \sigma(I)$]	0.0644 / 0.1697
Final R_1 / wR_2^a (all data)	0.1136 / 0.2005
Goodness-of-fit on F^2 ^b	1.024
Largest diff. peak / hole, e Å^{-3}	1.055 / –0.646

Table 1. Crystal and structure refinement data for $[\text{Mn}(\text{Mentb})(\text{salicylate})\text{DMF}](\text{NO}_3)$.

^a $R_1 = \sum |F_o| - |F_c| / \sum |F_o|$; $wR_2 = [\sum w(F_o^2 - F_c^2)^2 / \sum w(F_o^2)^2]^{1/2}$, $w = [\sigma^2(F_o^2) + (0.0963P)^2 + 1.0515P]^{-1}$, where $P = (\text{Max}(F_o^2, 0) + 2F_c^2) / 3$; ^b $\text{GoF} = S = [\sum w(F_o^2 - F_c^2)^2 / (n_{\text{obs}} - n_{\text{param}})]^{1/2}$, where n_{obs} is the number of data and n_{param} the number of refined parameters.

Bond lengths			
Mn–N1	2.537(3)	Mn–N3	2.201(4)
Mn–N5	2.294(3)	Mn–N7	2.273(4)
Mn–O1	2.249(3)	Mn–O2	2.420(3)
Mn–O7	2.285(4)		
Bond angles			
N3–Mn–O1	144.55(13)	N3–Mn–N7	119.52(13)
O1–Mn–N7	90.41(13)	N3–Mn–O7	82.44(14)
O1–Mn–O7	83.57(14)	N7–Mn–O7	82.11(14)
N3–Mn–N5	100.27(13)	O1–Mn–N5	89.48(12)
N7–Mn–N5	103.58(13)	O7–Mn–N5	171.08(14)
N3–Mn–O2	89.90(12)	O1–Mn–O2	55.91(11)
N7–Mn–O2	144.07(12)	O7–Mn–O2	81.95(14)
N5–Mn–O2	89.54(12)	N3–Mn–N1	70.66(12)
O1–Mn–N1	143.37(11)	N7–Mn–N1	68.07(12)
O7–Mn–N1	120.10(14)	N5–Mn–N1	68.70(11)
O2–Mn–N1	146.73(11)		

Table 2. Selected bond lengths (Å) and angles (deg) for [Mn(Mentb)(salicylate)DMF](NO₃).

diffractometer with graphite-monochromatized MoK α radiation ($\lambda = 0.71073$ Å) at 293 K. Data reduction and cell refinement were performed using the program SAINT [18], and an empirical absorption correction was performed using SADABS [19]. The structure was solved by Direct Methods and refined by full-matrix least-squares against F^2 using SHELXTL [20]. All H atoms were found in difference electron maps and were subsequently refined in a riding model approximation with C–H distances ranging from 0.93 to 0.97 Å and $U_{\text{iso}}(\text{H}) = 1.2 U_{\text{eq}}(\text{C})$. Crystal data and numbers pertinent to data collection and structure refinement are given in Table 1. Selected bond lengths and angles are listed in Table 2.

CCDC 870603 contains the supplementary crystallographic data for this paper. These data can be obtained free of charge from The Cambridge Crystallographic Data Centre via www.ccdc.cam.ac.uk/data_request/cif.

Results and Discussion

The nitrate of the Mn(II) complex is soluble in DMF and DMSO, but insoluble in water and organic solvents, such as methanol, ethanol, benzene, petroleum ether, trichloromethane, *etc.* The elemental analysis confirms its composition as [Mn(Mentb)(salicylate)DMF](NO₃).

The IR and UV spectra of the title complex are similar to that of the previously reported perchlorate salt of the Mn(II) complex [12]. The free ligand (Mentb) shows two strong bands at 1288 and 1477 cm⁻¹, attributable to $\nu(\text{C}=\text{N})$ and $\nu(\text{C}=\text{N})$ [21–23], but two strong bands are found for the complex at 1250 and 1458 cm⁻¹. These bands are shifted to lower frequencies by *ca.* 19–38 cm⁻¹ upon complex formation which implies direct coordination of the three imine ni-

trogen atoms to Mn(II). The complex shows two bands at 1593 and 1488 cm⁻¹ ($\Delta\nu = 105$ cm⁻¹) attributable to $\nu_{\text{as}}(\text{O}=\text{C}=\text{O})$ and $\nu_{\text{s}}(\text{O}=\text{C}=\text{O})$, indicating a bidentate coordination [24–26] of the salicylate anion [27]. The bands at 1388, 881 and 748 cm⁻¹ indicate that a nitrate anion (D_{3h}) is present [27].

Molecular structure of the complex

The ORTEP plot of the [Mn(Mentb)(salicylate)DMF] cation with the atom numbering adopted is shown in Fig. 1.

The asymmetric unit of the complex consists of a [Mn(Mentb)(salicylate)DMF] cation and a nitrate anion. The Mentb ligand forms a tripodal pyramidal geometry with the manganese ion, and the remaining coordination sites of the complex are occupied by a chelating salicylate anion and a monodentate DMF. The structure of the [Mn(Mentb)(salicylate)DMF] cation is similar to the previously reported one in the perchlorate [11, 12]. The bond length between the manganese ion and the apical nitrogen atom N1–Mn is 2.537(3) Å which is about 0.281 Å longer than the bond lengths between the manganese ion and the basal nitrogen atoms (2.201(4)–2.294(3) Å, average = 2.256 Å). This significant elongation has been observed in other manganese complexes with tripodal tetradentate ligands with a benzimidazolymethyl group [28]. The average bond angle NA–Mn–NB of the axial nitrogen atoms (NA = N1), the manganese ion, and the basal nitrogen atoms (NB = N3, N5, N7) is 69.14°, and the manganese ion is 0.801 Å above the trigonal basal plane. The oxygen atom of the monodentate DMF is coordinated in *trans* position to the basal

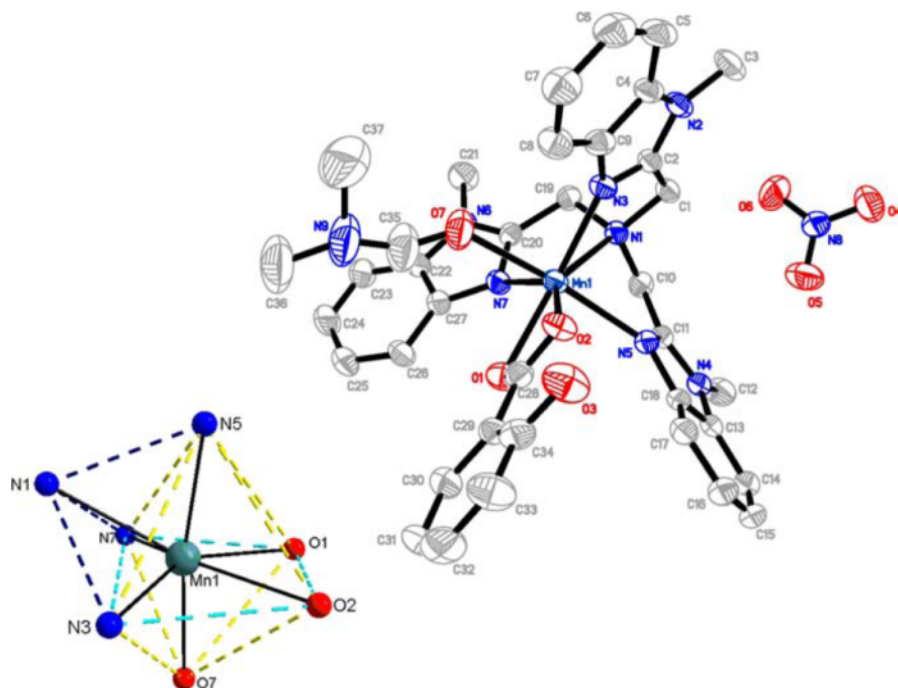


Fig. 1. Molecular structure of $[\text{Mn}(\text{Mentb})(\text{salicylate})\text{DMF}]\text{NO}_3$ with crystallographic atom numbering adopted (hydrogen atoms omitted for clarity) and a representation of the manganese coordination sphere (left).

N5 atom ($\text{N5-Mn-O7} = 171.08(14)^\circ$). The oxygen atoms of the chelating salicylate group are coordinated to the approximate *trans* positions of the remaining two basal nitrogen atoms ($\text{O1-Mn-N3} = 144.55(13)^\circ$, $\text{O2-Mn-N7} = 144.07(12)^\circ$). The additional ligands are accommodated at the opened axial site without significant change in the trigonal-pyramidal part of the complex ($\text{N3-Mn-N7} = 119.52(13)^\circ$). Steric crowding of the ligands is avoided because the manganese(II) ion is positioned slightly below the trigonal basal plane.

DNA-binding properties

Electronic absorption

The application of electronic absorption spectroscopy in DNA-binding studies has proven to be one of the most useful techniques [29]. Absorption titration experiments were performed with fixed concentrations of the complex, while gradually increasing the concentration of DNA. While measuring the absorption spectra, a proper amount of DNA was added to both the compound solution and the reference solution to eliminate the absorbance of DNA itself. In the UV region,

the intense absorption bands observed in the ligand and complex are attributed to *intra*-ligand $\pi-\pi^*$ transitions. From the absorption titration data, the binding constant was determined using the following equation [30]:

$$[\text{DNA}]/(\varepsilon_a - \varepsilon_f) = [\text{DNA}]/(\varepsilon_b - \varepsilon_f) + 1/K_b(\varepsilon_b - \varepsilon_f)$$

where $[\text{DNA}]$ is the concentration of DNA in base pairs, ε_a corresponds to the extinction coefficient observed ($A_{\text{obsd}}/[\text{M}]$), ε_f corresponds to the extinction coefficient of the free compound, ε_b is the extinction coefficient of the compound when fully bound to DNA, and K_b is the intrinsic binding constant. The ratio of slope to intercept in the plot of $[\text{DNA}]/(\varepsilon_a - \varepsilon_f)$ vs $[\text{DNA}]$ gives the values of K_b . The absorption spectra of the Mn(II) nitrate complex in the absence and presence of CT-DNA are given in Fig. 2.

With increasing DNA concentrations, the hypochromisms is 45.9% at 260 nm for the Mn(II) complex, suggesting that the Mn(II) complex interacts with CT-DNA [31]. The K_b value of the Mn(II) complex is $6.56 \times 10^4 \text{ L mol}^{-1}$ ($R = 0.9988$ for 15 points). Therefore, by comparison of these data with a DNA-intercalating ruthenium complex ($K_b = 1.1 \times 10^4 - 4.8 \times 10^4 \text{ L mol}^{-1}$) [32] one can

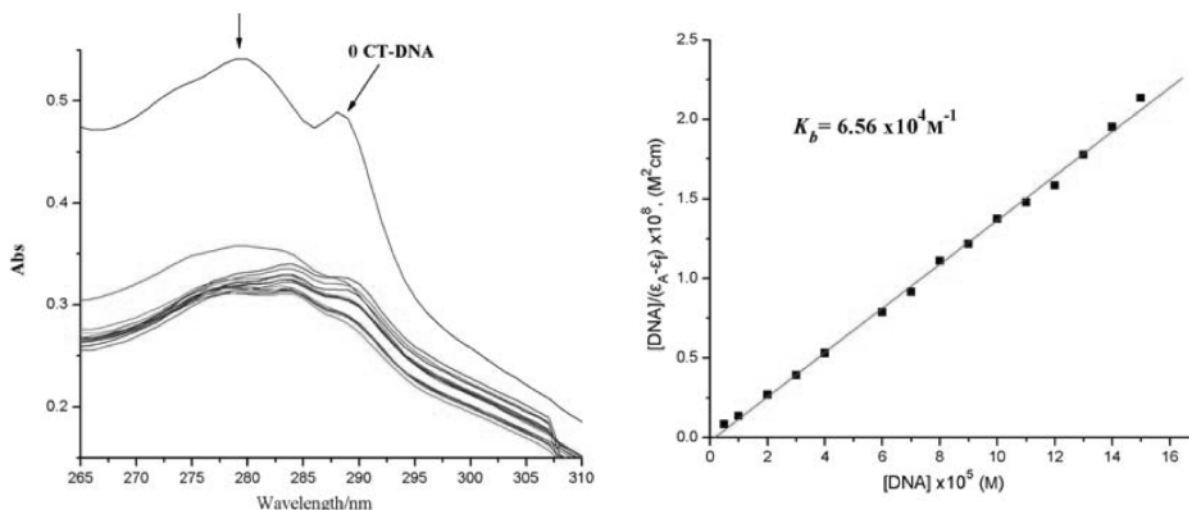


Fig. 2. Electronic spectra of the complex in Tris-HCl buffer upon addition of CT-DNA. $[\text{Complex}] = 3 \times 10^{-5} \text{ L mol}^{-1}$, $[\text{DNA}] = 2.5 \times 10^{-5} \text{ L mol}^{-1}$. The arrow shows the emission intensity changes upon increasing DNA concentration (left). Plots of $[\text{DNA}]/(\epsilon_a - \epsilon_f)$ vs. $[\text{DNA}]$ for the titration complex with CT-DNA (right).

conclude that the nitrate salt of the title Mn(II) complex most possibly binds to DNA in an intercalation mode.

Considering these experimental results, we speculate that the charge transfer of the ligand, caused by the coordination of the central Mn(II) atom, results in reduction of the charge density of the planar conjugated system. Therefore, the complex should bind to DNA more easily [33]. In addition, owing to the presence of an electron deficient center in the charged Mn(II) nitrate complex, an additional interaction between the complex and the phosphate-rich DNA backbone may be envisaged [34, 35].

Fluorescence spectra

No luminescence was observed for the complex at room temperature in aqueous solution, in any organic solvent examined, or in the presence of calf thymus (CT-DNA). So the binding of the complex cannot be directly observed in the emission spectra. The enhanced fluorescence of Ethidium bromide (EB) in the presence of DNA can be quenched by the addition of a second molecule [36, 37]. To further clarify the interaction of the complex with DNA, a competitive binding experiment was carried out in a buffer by keeping $[\text{DNA}]/[\text{EB}] = 1$ and varying the concentrations of the complex. The fluorescence spectra of EB were mea-

sured using an excitation wavelength of 520 nm. The emission range was set between 550 and 750 nm. The spectra were analyzed according to the classical Stern-Volmer equation [34, 38]:

$$I_0/I = 1 + K_{sv}[Q]$$

where I_0 and I are the fluorescence intensities at 599 nm in the absence and presence of the quencher, respectively, K_{sv} is the linear Stern-Volmer quenching constant, and $[Q]$ is the concentration of the Mn(II) complex. The fluorescence quenching of EB bound to CT-DNA by the complex is shown in Fig. 3.

In general, measurements of the ability of a complex to affect the intensity of an EB fluorescence in the EB-DNA adduct allow the determination of the affinity of the complex for DNA, whatever the binding mode may be. If a complex can displace EB from DNA, the fluorescence of the solution will be reduced due to the fact that free EB molecules are readily quenched by the solvent water [39]. For the nitrate salt of the Mn(II) complex, no emission was observed either alone or in the presence of CT-DNA in the buffer. The agreement with the Stern-Volmer equation provides further evidence that the compound binds to DNA. The K_{sv} value for the Mn(II) nitrate complex is $1.88 \times 10^4 \text{ L mol}^{-1}$ ($R = 0.9935$ for 16 points in the line part).

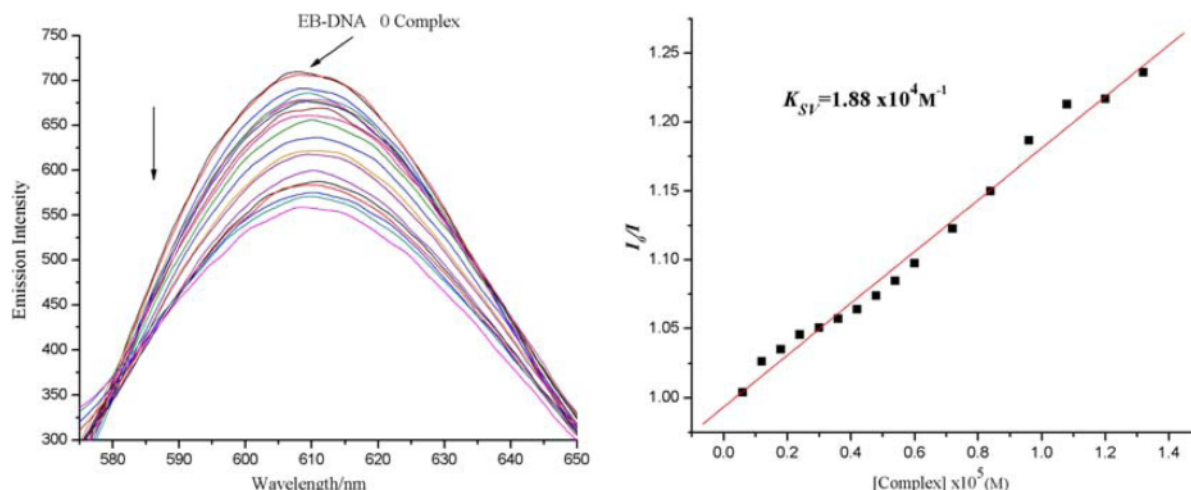


Fig. 3. Emission spectra of EB bound to CT-DNA in the presence of the complex (left). $[\text{Complex}] = 3 \times 10^{-5} \text{ L mol}^{-1}$; $\lambda_{\text{ex}} = 520 \text{ nm}$. The arrows show the intensity changes upon increasing the concentration of the complex (left). Plot I_0/I vs. $[\text{complex}] \times 10^5$ (right).

Viscosity measurements

Hydrodynamic measurements that are sensitive to changes in DNA length are regarded as the least ambiguous and most critical tests of a binding model in solution in the absence of crystallographic structural data [40, 41]. In classical intercalation, the DNA helix lengthens as base pairs are separated to accommodate the bound complex, leading to increased DNA viscosity, whereas a partial, non-classical complex intercalation causes a bend (or kink) of the DNA helix and reduces its effective length and thereby its viscosity [42]. Viscosity experiments were conducted with an Ubbelohde viscometer, immersed in a water bath maintained at 25.0 ± 0.1 °C. Titrations were performed for the complex ($3-30 \mu\text{M}$), the compound being introduced into the CT-DNA solution ($42.5 \mu\text{M}$) present in the viscometer. Data were analyzed as $(\eta/\eta_0)^{1/3}$ vs. the ratio of the concentration of the compound to CT-DNA, where η is the viscosity of CT-DNA in the presence of the compound and η_0 is the viscosity of CT-DNA alone. Viscosity values were calculated from the observed flow time of CT-DNA-containing solutions corrected for the flow time of buffer alone (t_0), $\eta = (t - t_0)$ [43].

The effect of the Mn(II) complex on the viscosity of CT-DNA are shown in Fig. 4. The viscosity of CT-DNA increased steadily with increasing amounts of the nitrate salt Mn(II) complex. It is further illustrated that

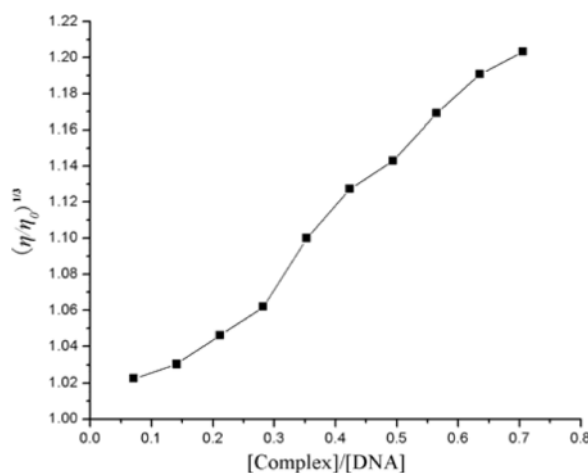


Fig. 4. Effect of increasing amounts of the complex on the relative viscosity of CT-DNA at 25.0 ± 0.1 °C.

the complex can intercalate with CT-DNA [44]. The results of the viscosity experiments confirm the mode of Mn(II) complex intercalation into DNA base pairs already established through absorption and fluorescence spectral studies.

Antioxidant activity

Hydroxyl radicals were generated in aqueous media through the Fenton-type reaction [13, 45]. The reaction mixture (3 mL) contained 1.0 mL of 0.10 mmol aque-

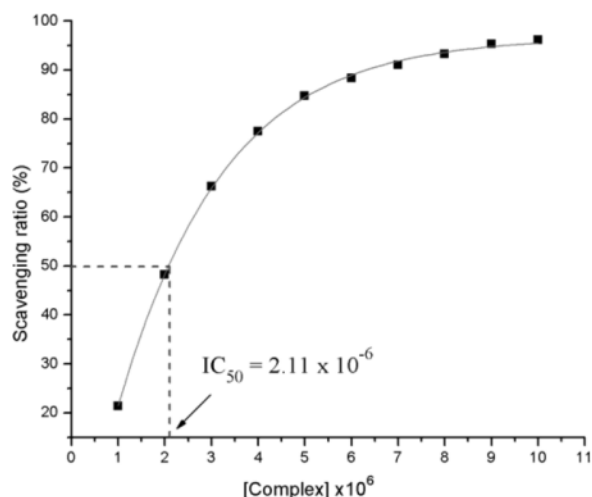


Fig. 5. The inhibitory effect of the complex on OH^\cdot radicals; the suppression ratio increases with the concentration of the test complex.

ous safranin, 1 mL of 1.0 mmol aqueous EDTA-Fe(II), 1 mL of 3% aqueous H_2O_2 , and a series of quantitative microadditions of solutions of the test compound. A sample without the tested compound was used as the control. The reaction mixtures were incubated at 37°C for 30 min in a water bath. The absorbance was then measured at 520 nm. All the tests were run in triplicate and are expressed as the mean and standard deviation (SD) [46]. The scavenging effect for OH^\cdot radical was calculated from the following expression:

$$\text{Scavenging ratio (\%)} = [(A_i - A_0)/(A_c - A_0)] \times 100$$

where A_i = absorbance in the presence of the test compound, A_0 = absorbance of the blank in the absence of the test compound, A_c = absorbance in the absence of the test compound, EDTA-Fe(II) and H_2O_2 .

We compared the ability of the present compound to scavenge hydroxyl radicals with those of the well-known natural antioxidants mannitol and vitamin C,

using the same method as reported in a previous paper [47]. The 50% inhibitory concentration (IC_{50}) values of mannitol and vitamin C are about 9.6×10^{-3} and $8.7 \times 10^{-3} \text{ M}^{-1}$, respectively. According to the antioxidant experiments, the IC_{50} values of the nitrate salt of the Mn(II) complex is $2.11 \times 10^{-6} \text{ M}^{-1}$ (Fig. 5), which implies that the complex exhibits better scavenging activity than mannitol and vitamin C.

Conclusions

In previous work we reported on the monocationic seven-coordinate Mn(II) complex $[\text{Mn}(\text{Mentb})(\text{salicylate})\text{DMF}]^+$ as its perchlorate containing tris(2-(*N*-methyl)benzimidazolylmethyl)amine, salicylate and DMF as ligands. Based on that work, the same Mn(II) complex was synthesized as nitrate, and the binding modes of the Mn(II) complex with CT-DNA were studied. Especially photophysical and viscosity measurements indicated that the Mn(II) complex interacts with CT-DNA through intercalative binding, which may be due to charge transfer and reduction of the charge density of the planar conjugated system upon coordination to the metal complex. The hydroxyl radical scavenging potential of the complex was also investigated, and the results show that the Mn(II) complex exhibits effective scavenging properties. These findings indicate that the Mn(II) complex has many potential practical applications for the development of nucleic acid molecular probes and new therapeutic reagents for diseases on the molecular level and warrants further *in vivo* experiments and pharmacological assays.

Acknowledgement

The authors acknowledge the financial support and a grant from 'Qing Lan' Talent Engineering Funds by Lanzhou Jiaotong University. A grant from 'Long Yuan Qing Nian' of Gansu Province also is acknowledged.

- [1] V. S. Li, D. Choi, Z. Wang, L. S. Jimenez, M. S. Tang, H. Kohn, *J. Am. Chem. Soc.* **1996**, *118*, 2326–2331.
- [2] G. Zuber, J. C. Quada, Jr., S. M. Hecht, *J. Am. Chem. Soc.* **1998**, *120*, 9368–9369.
- [3] J. K. Barton, *Science* **1986**, *233*, 727–734.
- [4] K. E. Erkkila, D. T. Odom, J. K. Barton, *Chem. Rev.* **1999**, *99*, 2777–2795.
- [5] V. L. Pecoraro (Ed.), *Manganese Redox Enzymes*, VCH Publishers, New York **1992**.
- [6] K. Wieghardt, *Angew. Chem., Int. Ed. Engl.* **1989**, *28*, 1153–1172.
- [7] V. L. Pecoraro, M. J. Baldwin, A. Gelasco, *Chem. Rev.* **1994**, *94*, 807–826.
- [8] R. J. Sundberg, R. B. Martin, *Chem. Rev.* **1974**, *74*, 471–517.
- [9] D. S. Pilch, Z. Xu, Q. Sun, E. J. Lavoie, L. F. Liu, N. E. Geacintov, K. J. Breslauer, *Drug Des. Discov.* **1996**, *13*, 115–133.

- [10] B. Willis, D. P. Arya, *Biochem.* **2010**, *49*, 452–469.
- [11] H. L. Wu, Y. Bai, X. C. Huang, X. Meng, B. L. Qi, *Acta Crystallogr.* **2010**, *E66*, m1252.
- [12] H. L. Wu, F. Jia, X. Meng, Q. Chen, B. Liu, Y. L. Lai, F. Kou, *J. Coord. Chem.* **2010**, *63*, 3627–3634.
- [13] S. Satyanaryana, J. C. Dabrowiak, J. B. Chaires, *Biochem.* **1993**, *32*, 2573–2584.
- [14] J. Marmur, *J. Mol. Biol.* **1961**, *3*, 208–218.
- [15] H. M. J. Hendriks, P. J. M. W. L. Birker, G. C. Verschoor, J. Reedijk, *J. Chem. Soc., Dalton. Trans.* **1982**, 623–631.
- [16] W. K. Dong, Y. X. Sun, C. Y. Zhao, X. Y. Dong, L. Xu, *Polyhedron* **2010**, *29*, 2087–2097.
- [17] W. K. Dong, C. Y. Zhao, Y. X. Sun, X. L. Tang, X. N. He, *Inorg. Chem. Commun.* **2009**, *12*, 234–236.
- [18] SAINT, Bruker Analytical X-ray Instruments Inc., Madison, Wisconsin (USA) **2000**.
- [19] G. M. Sheldrick, SADABS, Program for Empirical Absorption Correction of Area Detector Data, University of Göttingen, Göttingen (Germany) **2004**.
- [20] G. M. Sheldrick, SHELXTL, Siemens Analytical X-ray Instruments Inc., Madison, Wisconsin (USA) **1996**. See also: G. M. Sheldrick, *Acta Crystallogr.* **2008**, *A64*, 112–122.
- [21] C. Y. Su, B. S. Kang, C. X. Du, Q. C. Yang, T. C. W. Mak, *Inorg. Chem.* **2000**, *39*, 4843–4849.
- [22] T. J. Lane, I. Nakagawa, J. L. Walter, A. J. Kandathil, *Inorg. Chem.* **1962**, *1*, 267–276.
- [23] A. W. Addison, H. M. J. Hendriks, J. Reedijk, L. K. Thompson, *Inorg. Chem.* **1981**, *20*, 103–110.
- [24] P. P. Hankare, S. R. Naravane, V. M. Bhuse, S. D. Deleker, A. H. Jaytap, *Indian J. Chem.* **2004**, *43*, 1464–1467.
- [25] K. Nakamoto, *Infrared and Raman Spectra of Inorganic and Coordination Compounds*, Vol. 3, John Wiley and Sons, Academic Press, New York, **1978**, pp. 200–201.
- [26] J. Catterick, P. Thornton, *Adv. Inorg. Chem.* **1977**, *20*, 291–362.
- [27] S. Musumeci, E. Rizzarelli, S. Sammartano, A. Seminaba, *Z. Anorg. Allg. Chem.* **1977**, *433*, 297–304.
- [28] M. S. Lah, H. Chun, *Inorg. Chem.* **1997**, *36*, 1782–1785.
- [29] H. L. Wu, Y. C. Gao, *Trans. Met. Chem.* **2004**, *29*, 175–179.
- [30] Z. X. Su, Y. Q. Wan, H. L. Wu, *Synth. React. Inorg. Met. Org. Nano. Met. Chem.* **2005**, *35*, 553–558.
- [31] K. Byunghoon, W. C. Ki, P. Myungho, S. L. Myoung, *Inorg. Chim. Acta* **1999**, *290*, 21–27.
- [32] J. K. Barton, A. Danishefsky, J. Goldberg, *J. Am. Chem. Soc.* **1984**, *106*, 2172–2176.
- [33] H. L. Wu, F. Kou, F. Jia, B. Liu, J. K. Yuan, Y. Bai, *J. Photochem. Photobiol. B* **2011**, *105*, 190–197.
- [34] A. Wolfe, G. H. Shimer, Jr., T. Meehan, *Biochem.* **1987**, *26*, 6392–6396.
- [35] J. Liu, T. X. Zhang, L. N. Ji, *J. Inorg. Biochem.* **2002**, *91*, 269–276.
- [36] A. M. Pyle, J. P. Rehmann, R. Meshoyrer, C. V. Kumar, N. J. Turro, J. K. Barton, *J. Am. Chem. Soc.* **1989**, *111*, 3051–3058.
- [37] S. Yellappa, J. Seetharamappa, L. M. Rogers, R. Chitta, R. P. Singhal, F. D'Souza, *Bioconjugate Chem.* **2006**, *17*, 1418–1425.
- [38] M. Shakir, M. Azam, M.-F. Ullah, S.-M. Hadi, *J. Photochem. Photobiol. B.* **2011**, *104*, 449–456.
- [39] B. C. Baguley, M. Le Bret, *Biochem.* **1984**, *23*, 937–943.
- [40] J. R. Lakowicz, G. Webber, *Biochem.* **1973**, *12*, 4161–4170.
- [41] M. Chauhan, K. Banerjee, F. Arjmand, *Inorg. Chem.* **2007**, *46*, 3072–3082.
- [42] J. B. LePecq, C. Paoletti, *J. Mol. Biol.* **1967**, *27*, 87–106.
- [43] M. Sethuraman, P. Mallayan, *Inorg. Chem.* **1998**, *37*, 693–700.
- [44] A. B. Tossi, J. M. Kelly, *Photochem. Photobiol.* **1989**, *49*, 545–556.
- [45] C. P. Tan, J. Liu, L. M. Chen, S. Shi, L. N. Ji, *J. Inorg. Biochem.* **2008**, *102*, 1644–1653.
- [46] S. Satyanarayana, J. C. Dabrowiak, J. B. Chaires, *Biochem.* **1992**, *31*, 9319–9324.
- [47] T. R. Li, Z. Y. Yang, B. D. Wang, D. D. Qin, *Eur. J. Med. Chem.* **2008**, *43*, 1688–1695.